Journal of Inorganic Biochemistry 203 (2020) 110873

Contents lists available at ScienceDirect

Journal of Inorganic Biochemistry

journal homepage: www.elsevier.com/locate/jinorgbio

Effects of vanadium(IV) compounds on plasma membrane lipids lead to G protein-coupled receptor signal transduction

Duaa Althumairy[a,d], Heide A. Murakami[b], Dongmei Zhang[b], B. George Barisas[a,b], Deborah A. Roess[c,**], Debbie C. Crans[a,b,*]

[a] Cell and Molecular Biology Program, Colorado State University Fort Collins, CO 80523, United States of America
[b] Department of Chemistry, Colorado State University Fort Collins, CO 80523, United States of America
[c] Department of Biomedical Sciences, Colorado State University Fort Collins, CO 80523, United States of America
[d] Department of Biological Sciences, King Faisal University, Saudi Arabia

ARTICLE INFO

Keywords:
Vanadium
G-protein-coupled receptor
BMOV
Signal transduction
Vanadyl
Plasma membrane rafts
Luteinizing hormone receptor

ABSTRACT

Luteinizing hormone receptors (LHR), expressed at physiological numbers < 30,000 receptors per cell, translocate to and signal within membrane rafts following binding of human chorionic gonadotropin (hCG). Similarly LHR signal in cells when treated with bis(maltolato)oxovanadium(IV) (BMOV), bis(ethylmaltolato)oxovanadium (IV) (BEOV) or $VOSO_4$, which decrease membrane lipid packing. Overexpressed LHR (> 85,000 receptors per cell) are found in larger clusters in polarized homo-transfer fluorescence resonance energy transfer (homo-FRET) studies that were not affected by either hCG or vanadium compounds. Intracellular cyclic adenylate monophosphate (cAMP) levels indicate that only clustered LHR are active and produce the intracellular second messenger, cAMP. When LHR are over-expressed, cell signaling is unaffected by binding of hCG or vanadium compounds. To confirm the existence of intact complex, the EPR spectra of vanadium compounds in cell media were obtained using 1 mM BMOV, BEOV or $VOSO_4$. These data were used to determine intact complex in a 10 μM solution and verified by speciation calculations. Effects of BMOV and BEOV samples were about two-fold greater than those of aqueous vanadium(IV) making it likely that intact vanadium complex are responsible for effects of LHR function. This represents a new mechanism for activation of a G protein-coupled receptor; perturbations in the lipid bilayer by vanadium compounds lead to aggregation and accumulation of physiological numbers of LHR in membrane raft domains where they initiate signal transduction and production of cAMP, a second messenger involved in signaling.

1. Introduction

Vanadium compounds [1–4] and salts [2,3,5] have been reported to have antidiabetic properties [2,3,6–9], anticancer properties [10–13], cardioprotective properties [1,14,15] as well other beneficial effects on other diseases [14,16,17]. Studies have been dedicated to both understanding the fundamental biochemical processing in various biological systems [18–22], toxicity [19,21], as well as applications combatting diseases [1,22]. Interestingly, vanadyl sulfate ($VOSO_4$), sodium metavanadate ($NaVO_3$) and a coordination complex bis(ethylmaltolato)oxovanadium(IV) (BEOV) are vanadium compounds having insulin-like activity [3,22–24]. Both the salts [10,22] and BEOV [23,24] (Fig. 1) have been considered for human use as an antidiabetic agents. Furthermore, the biological effects of these salts as well as bis(maltolato) oxovanadium(IV) (BMOV) have been extensively studied (Fig. 1), with many reports describing its interactions in biological systems [3,6,19,23]. Many modes of interactions of various vanadium compounds have been identified including inhibition of protein phosphatases [25–27], interactions with circulating proteins such as serum albumin and transferrin [19,28], effects on reactive oxygen species (ROS) levels [16,29,30] as well as less well known effects of vanadium compounds on the plasma membrane [31].

The plasma membrane and its lipids can be considered as a drug target. Changes in membrane lipid composition or alterations in membrane lipid microenvironments can affect signal transduction by G protein-coupled receptors through direct or indirect effects on the receptor's local lipid environment [32,33]. Although most drugs will need to enter cells, a few compounds that interact with membrane lipids

* Correspondence to: Debbie C. Crans, Cell and Molecular Biology Program, Colorado State University Fort Collins, CO 80523, United States of America.
** Corresponding author.
E-mail address: Debbie.Crans@colostate.edu (D.C. Crans).

https://doi.org/10.1016/j.jinorgbio.2019.110873
Received 10 June 2019; Received in revised form 27 September 2019; Accepted 27 September 2019
Available online 22 October 2019
0162-0134/

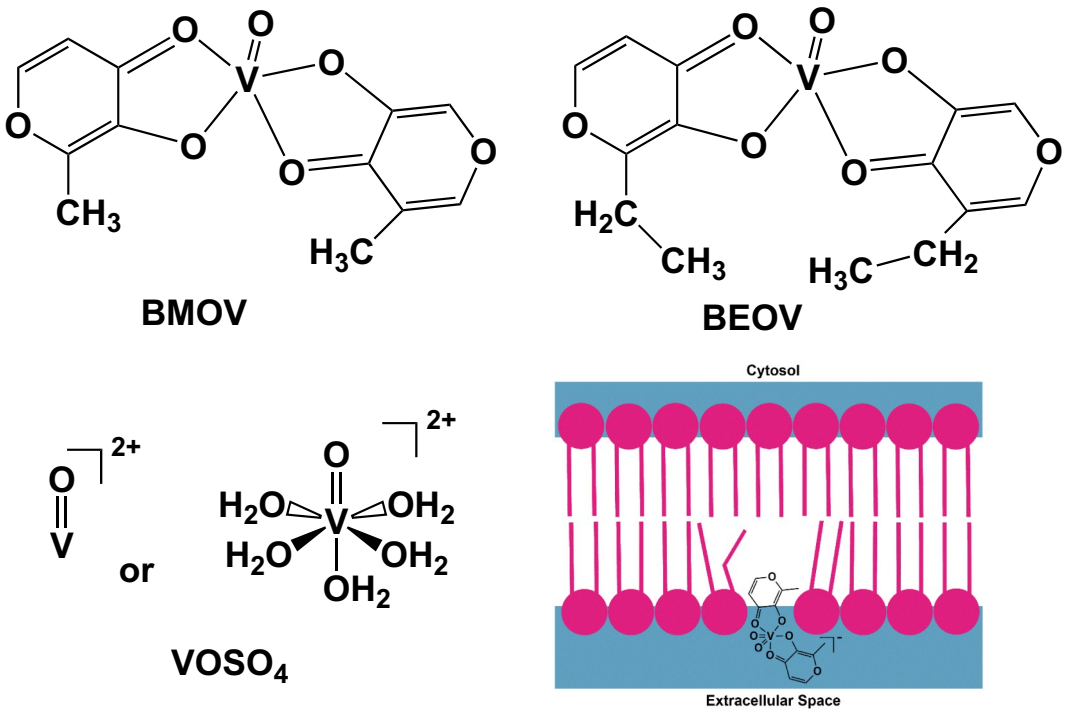

Fig. 1. Structures of BMOV, BEOV, vanadyl sulfate ($VOSO_4$) and a schematic of a lipid bilayer with a molecule of BMOV.

Table 1
Historical summary of plasma membrane studies and interaction of membrane lipids with vanadium compounds.

1972	Singer and Nicolson propose the fluid mosaic model [41]
1985	Lateral diffusion of LHRs is affected by ligand binding [42]
1992	LHR undergo aggregation upon binding of hormone [43]
1997	Lipid rafts are identified as specialized membrane microdomains [34]
2000	Lipid rafts concentrate proteins involved in signal transduction by Type I Fcε receptors [38] and insulin receptors (IR) [39]
2003	IR activation is decreased when IR cannot access the rafts [40]
2005	The anionic dipicolinatobisoxovanadium(V) [VO_2dipic]$^-$) is found to interact with a positively charged model membrane interface [44]
2006	[VO_2dipic]$^-$ is found to penetrate a negatively charged model membrane interface [45]
2007	RBL-2H3 cells, a basophil-derived cell line, undergo release of histamine from cell vesicles following exposure to VO(saltris)$_2$, a response characteristic of Type I Fcε receptor aggregation [46]
2008	VO(saltris)$_2$ causes translocation of IR in raft domains in RBL-2H3 cells [47]
2008	BMOV-treated cells undergo Ca^{2+} flux when RBL-2H3 cells are treated with DNP-BSA, a polymeric antigen that crosslinks Type I Fcε receptors [47]
2008	BMOV is found to interact with the negatively charged model membrane interface [48]
2011	Bis(maltolato)dioxovanadium(V) ([VO_2(malto)$_2$]$^-$) is found to hydrolyze as it approaches and interact with the negatively charged model membrane interfaces
2012	BMOV drives reorganization of the plasma membrane and IR activation in lipid rafts [30]
2012	Chromium(III) picolinate and insulin cause increased IR confinement in RBL-2H3 plasma membrane microdomains [49]
2013	Decavanadate causes histamine release from RBL-2H3 cells through effects on membrane lipids and facilitation of Type 1 Fcε receptor-mediated signaling [50]
2014	Interactions with model membrane interfaces and compound uptake are correlated for different V-dipicolinate derivatives [51]

without entering the cell may have pharmacological activity. The interactions of two vanadium compounds and $VOSO_4$ with mammalian cell membrane lipids, shown here, appears to result in hormone-like effects on LHR accumulation in plasma membrane rafts and receptor signal transduction in the absence of hormone signals.

Membrane lipid microdomains such as lipid rafts are critical in the function of many plasma membrane receptors including luteinizing hormone receptors (LHR). Rafts are plasma membrane structures that are enriched with cholesterol, sphingolipids, lipid-anchored molecules and select transmembrane proteins [34]. Signaling complexes associated with membrane rafts form on the membrane cytoplasmic face upon receptor aggregation and actively transduce signal. Like other G protein-coupled receptors, LHR bind ligand to extracellular receptor structures and transduce signal across the membrane via a conformational change in their seven transmembrane helices. Interactions between intracellular receptor structures and G proteins lead to G protein activation and activation of intracellular signaling cascades. As part of hormone-induced signaling, LHR translocate to plasma membrane microdomains after binding of human chorionic gonadotropin (hCG) [35]. LHR exhibit slower rotational diffusion on intact cells [36] and membrane fragments [37], both suggesting receptor aggregation into large molecular weight structures within raft microdomains. It is believed that these membrane microdomains concentrate membrane proteins involved in signal transduction as is the case for Type I Fcε receptors involved in the immune system response to allergens [38] and insulin receptors (IR) [39]. IR are unable to access raft microdomains after crosslinking of GM-1, a raft component, and this, in turn blocks IRS-1 activation by ligand-bound IR [40].

Although BMOV and BEOV have been found to associate with membrane models, they have also be found to hydrolyze as they approach the interface in a model system and form VO^{2+} [48]. The structures of BMOV, BEOV and VO^{2+} are shown in Fig. 1 together with proposed interactions of oxidized BMOV with plasma membrane lipids based on reported studies with a model membrane interface [48]. Insulin-like activity of BMOV have been inferred to result from direct effects of BMOV on the organization of plasma membrane lipids [31].

BMOV interactions with membrane lipids was accompanied by translocation of IR from the bulk membrane to membrane microdomains where receptors signaled without addition of the receptor ligand.

In Table 1 we summarize the contributions to this field beginning from Singer and Nicolson's fluid mosaic model of the plasma membrane to the studies presented in this work exploring the effects of BMOV on IR signal transduction. A tabulation of findings with regard to the properties of lipid membranes and the effects vanadium compounds exert on membrane organization and properties was done to compare the information regarding the properties in the presence and absence of lipid-like compounds.

The question addressed in this manuscript concerns whether LHR initiates signal transduction in cells treated with BMOV, BEOV or $VOSO_4$ and whether vanadium compound effects occur only when cells expressing physiologically low numbers of LHRs are capable of signaling in response to hormone. *We hypothesize that vanadium-containing compounds can have hormone-like activity resulting from their interactions with membrane lipids in cells expressing low numbers of receptors.* This effect of the vanadium compounds is due to a sequence of events that involves BMOV, BEOV or $VOSO_4$ interactions with membrane lipids, an increased preference of LHR for raft domains and aggregation of receptors leading to signaling in the absence of hCG. We have developed a model describing hormone and vanadium compound effects on LHR signal transduction (Fig. 2). BMOV, BEOV and VOSO4 effects are limited to cells expressing physiologically relevant numbers of LHR. When cells express higher numbers of LHR per cell, receptors are already aggregated and actively signaling in raft domains. The addition of either vanadium compounds or hCG has no further effect on receptor aggregation or receptor-mediated signaling.

2. Materials and methods

2.1. General methods

Chinese Hamster Ovary cells CHO-K1 were kindly provided by Dr. Takamitsu Kato at Colorado State University. Dulbecco's Modified Eagle medium (DMEM) and geneticin were purchased from Corning Cellgro. Penicillin/streptomycin and L-glutamine solution were purchased from Gemini Bio-Products (West Sacramento, CA). Fetal bovine serum (FBS) was purchased from Atlas Biologicals (Fort Collins, CO). 100× MEM non-essential amino acid solution, bovine albumin, ethylenediaminetetraacetic acid (EDTA), methyl-β-cyclodextrin (MβCD), forskolin, MDL-12,330a hydrochloride and $VOSO_4$ were purchased from Sigma-Aldrich (St. Louis, MO). Trypsin-EDTA (0.25%) was purchased from Fisher Scientific Co (Pittsburgh, PA). Rhodamine 6G was purchased from Eastman Kodak (Rochester, New York). Lipofectamine 3000 was purchased from Life Technologies (Carlsbad, CA). Quantum FITC MESF (molecules of equivalent soluble fluorophore) beads were purchased from Bangs Laboratories (Fishers, IN). Optimal-MEM™ was purchased from Life Technologies (Carlsbad, CA). Human chorionic gonadotropin (hCG) was purchased from Fitzgerald Industries (Acton, MA). 35 mm diameter glass-bottom cell culture dishes were purchased from In Vitro Scientific (Sunnyvale, CA).

2.2. Stock solutions of BMOV, BEOV and $VOSO_4$

BMOV and BEOV were prepared as reported previously [48,52] using starting materials (maltol, ethylmaltol and $VOSO_4$) purchased from Sigma and Aldrich. The properties of these compounds in EPR and UV-VIS spectroscopy [48,52] and their stability in cell culture media

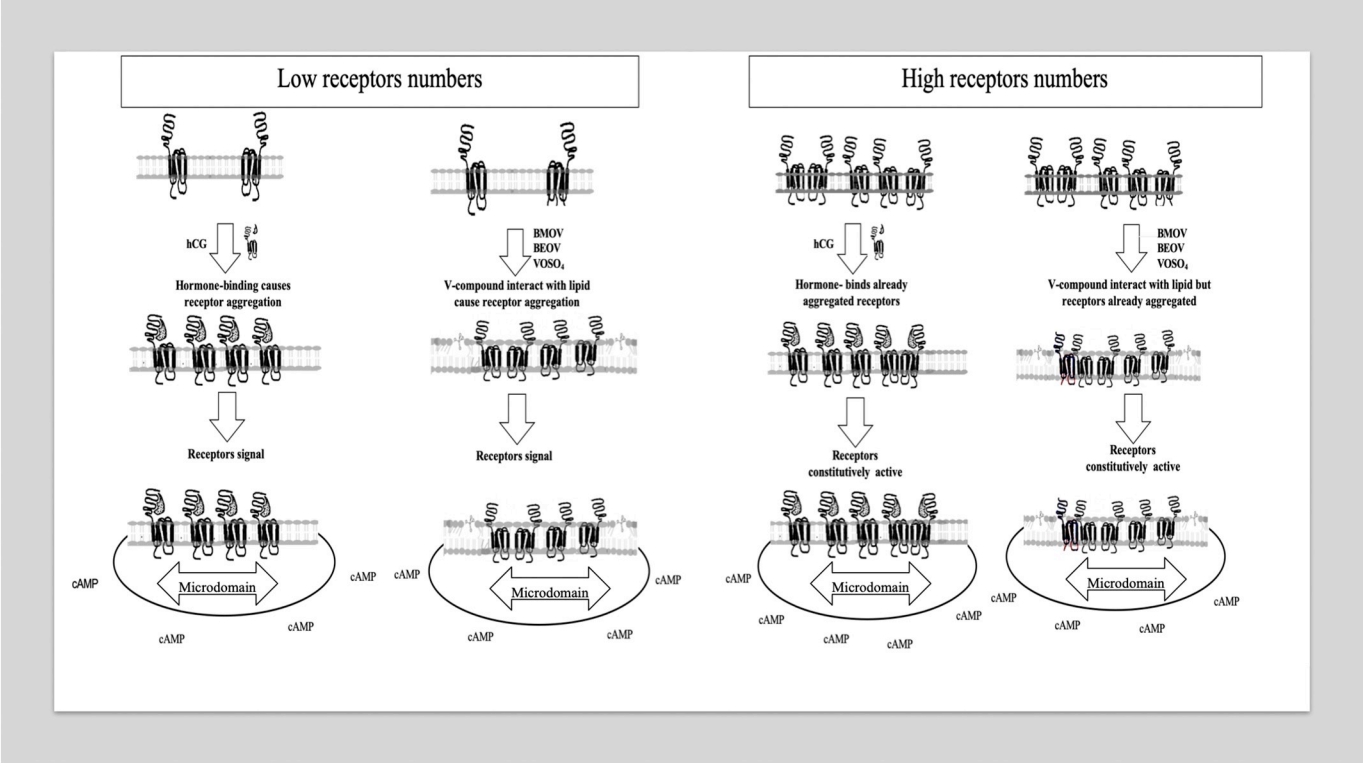

Fig. 2. Effects of low and high receptor numbers per cell on response to hormone or treatment with BMOV, BEOV or $VOSO_4$. Only upon binding of hCG (far left panel) do cells expressing low numbers of LHR per cell exhibit receptor clustering in plasma membrane microdomains. Vanadium compounds interact with the extracellular surface of the lipid bilayer (see Fig. 1) and produce LHR clustering similar to that seen following hCG binding to its receptor. Upon receptor clustering in response to hCG or vanadium compounds, anisotropy values for LHR-eYFP decrease, receptors initiate signal transduction and intracellular cAMP levels rise. In cells expressing high numbers of LHR (right panels) where receptor density may by > 10-fold higher than in cells expressing < 9 K receptors per cell, LHR are already clustered and are constitutively active. The LHR-eYFP anisotropy is low and basal intracellular cAMP levels are high. Addition of hCG or vanadium compounds has minimal effects on further clustering of the receptor or on intracellular cAMP levels.

[53] have been previously described. Stock solutions of 1 mM BMOV and BEOV were prepared by dissolving the BMOV and BEOV in powder form in < 0.5% DMSO and then adding phosphate buffered saline containing 1 mM $CaCl_2$ and 0.5 mM $MgCl_2$. A stock solution of $VOSO_4$ was made by dissolving the powder $VOSO_4$ in PBS. For homo-FRET, dilution of stock solutions into serum-free media (500 mL of DMEM, 5 mL of 100× non-essential amino acid solution, 5 mL of penicillin/streptomycin and 5 mL of L-glutamine solution) to get 10 mM were done immediately before beginning cell studies. In measurements of intracellular cAMP, stock solutions were diluted with PBS to final concentrations of 10 μM BMOV, 10 μM BEOV or 10 μM $VOSO_4$ with pH values between 7.3 and 7.4.

2.3. Preparation of cell lines stably expressing LHR-enhanced yellow fluorescent protein (eYFP)

To prepare CHO cells stably expressing known numbers of LHR per cell, CHO cells were transfected with 0.5 μg/μL of hLHR-eYFP using Lipofectamine 3000 in accordance with Manufacturer's instructions. The plasmid containing the entire coding region of the human LHR subcloned into pEYFP-N1, was kindly prepared by Dr. Ying Lei [54]. A microcentrifuge tube containing 125 μL of optimal-MEM Media and 7.5 μL Lipofectamine 3000 reagent was mixed with the contents of a second microcentrifuge tube containing 250 μL of Optimal-MEM media, 2.5 μg/μL of hLHR-eYFP and 2 μL/μg DNA in Lipofectamine 3000 and incubated at room temperature for 10–15 min. This mixture was added to CHO cells in one well of a 6 well plate and incubated for 24–48 h. For the stable cell line selection, the Optimal-MEM media was replaced with media containing G418 for 2–3 weeks post-transfection at which time cells had been selected that stably incorporated hLHR-eYFP plasmid into their genomic DNA. Stable cell lines were maintained in DMEM with 10% FBS, 1% penicillin and streptomycin, 1% L-glutamine, 1% 1× non-essential amino acids and 200 μg/mL of geneticin. Untransfected CHO cells were maintained in DMEM with 10% FBS, 1% penicillin/streptomycin, 1% L-glutamine and 1% 1× non-essential amino acids. All cells were maintained in 5% CO_2 at 37 °C.

2.4. Measurement of numbers of LHR-eYFP expressed per cell

Cells were grown to 80–90% confluence in 25 cm^2 culture flasks and then incubated with 1.0 mL trypsin-EDTA (0.25%) for 3 min before the flask was gently washed with 3 mL of 1× PBS. A 3 mL volume of cells at a concentration of 10^5–10^6 cells per mL was placed in a 5 mL VWR polypropylene tube for analysis using a Moflo Astrios EQ flow cytometer. Fluorescence intensity per cell was collected using 488 nm argon ion laser excitation and a 525/40 nm emission filter.

There are no bead standards for eYFP. However, the number of eYFP molecules expressed per cell can be determined from calibrations based on FITC bead standards. We denote the detected fluorescence signal in photons per second for one FITC chromophore on a calibration bead as R_{FITC} and the signal from a single eYFP as R_{YFP}. From photophysical properties of the chromophores and from cytometer instrumental parameters, we determined that the ratio R_{YFP}/R_{FITC} was 1.36. Thus, the number of eYFP per cell was 1.36× the number that would be inferred from FITC bead standards:

$$n_{YFP} = n_{FITC}\left(R_{YFP}/R_{FITC}\right) \quad (1)$$

2.5. Polarized homo-fluorescence resonance energy transfer (homo-FRET) measurements

Stable cell lines were grown to 80–90% confluence in 25 cm^2 culture flasks and then incubated with 1.0 mL trypsin-EDTA (0.25%) for 3 min. Cells (0.5 mL) were plated in a 35 mm glass-bottom petri dish. After 12 h, the cells were washed twice with 1× phosphate buffered saline (PBS; pH 7.3) and then suspended in medium with the appropriate treatment. Cells were incubated with 100 nM hCG or 10 mM MβCD for 1 h or with 10 μM BMOV, 10 μM BEOV or 10 μM $VOSO_4$ for 12 h. After taking the dishes from the incubator, cells were washed once, resuspended in PBS and immediately imaged with a Zeiss Axiovert 200 M inverted microscope. For untreated cells, the cell pellet was resuspended in 600 mL of PBS alone.

Energy transfer between chromophores of the same type is termed "homo-FRET" and occurs to a significant extent when donor eYFP and acceptor eYFP moieties are within 2–10 nm of each other [55]. In these studies, homo-FRET imaging data were collected using a Zeiss Axiovert 200 M inverted microscope with an Andor Du897E EMCCD camera and MetaMorph software. Arc lamp illumination passing through a vertically-polarized filter provided polarized excitation. Approximately 16 images were acquired at a rate of one image per minute with a 15 s exposure time. This exposure typically bleached eYFP to ~10% of its initial fluorescence intensity. A Princeton Instruments Dual View image splitter created simultaneously, and on the same image frame, side-by-side images of fluorescence polarized parallel and perpendicular to the excitation polarization. Backgrounds were subtracted from fluorescence emission images and a g-factor was calculated to correct for efficiency differences in instrument optics. Image J software was used for calculation of the g-factor as previously described [56,57].

The g-factor constitutes the instrument-specific correction for different detection sensitivities for vertically- and horizontally-polarized fluorescence. This can be evaluated using aqueous solutions that have anisotropy values near zero such as rhodamine 6G which has an anisotropy value of about 0.012 [56,57]. The g-factor is calculated by the following Eq. (2) [56] where I_{vv} and I_{vh} refer to measurements on a dilute rhodamine 6G solution and r_{R6G} is the literature value for rhodamine 6G anisotropy.

$$g = \frac{I_{vv}}{I_{vh}}\frac{(1 - r_{R6G})}{(1 + 2r_{R6G})} \quad (2)$$

The fluorescence intensities parallel and perpendicular to that of the exciting light, I_{vv} and I_{vh}, respectively, were used to calculate anisotropies using Eq. (3). The intrinsic anisotropy r_{YFP} of a single eYFP fluorophore is 0.38 [58]. We assumed monomeric LHR-eYFP exhibited this value and so set to 0.38 the apparent anisotropy upon complete bleaching. About 5–7 cells were examined from each petri dish and at least 30 cells were examined for each treatment. To avoid internalization of LHR-eYFP, data were acquired after no > 30 min.

$$r = \frac{(I_{vv} - gI_{vh})}{(I_{vv} + 2gI_{vh})} \quad (3)$$

2.6. Measurements of intracellular cAMP levels using the ICUE3 reporter

ICUE3 is based on a single cyclic nucleotide-binding domain based on the Epac probe, Epac1 149−881, fused to an enhanced cyan fluorescent protein (CFP) and a circularly-permuted Venus cpV-L194 [59]. In the absence of cAMP, the probe is folded with CFP close to the Venus eYFP. There is thus substantial energy transfer from CFP to eYFP, causing sensitized emission from eYFP. cAMP binding unfolds the probe, reducing FRET and causing an accompanying increase in CFP emission and a decrease in eYFP sensitized emission. The ratio of CFP fluorescence intensity to that of eYFP sensitized fluorescence intensity thus increases monotonically with cAMP concentration CHO cells stably expressing LHR were transiently transfected with 0.4 μg of cAMP level reporter ICUE3 plasmid provided by Dr. Jin Zhang as previously described [59]. During transfection, cells were maintained in 5% CO_2 at 37 °C for 24–48 h. Cells were then plated in a 35 mm glass bottom petri dishes for 12 h at which time cells were washed twice with 1× PBS, pH 7.3, and then suspended in PBS. Images were acquired first with PBS to establish baseline levels of intracellular cAMP. Then the cell media

was exchanged with solutions containing 100 nM hCG, 10 mM MβCD, 50 μM forskolin, 10 μM MDL-12,330a hydrochloride, 10 μM BMOV, 10 μM BEOV or 10 μM $VOSO_4$ for 15 min.

Images were acquired used a 63 × 1.2 NA water objective in a Zeiss Axiovert 200 M inverted microscope with an Andor Du897E EMCCD camera. Images were acquired using an arc lamp with a 436DF20 excitation filter and two emission filters, 480DF40 for CFP and 535DF30, for eYFP and eYFP sensitized emission (YFPSE) due to energy transfer from CFP. All filters were from Chroma Technology. MetaFluor software was used to observe and image cells during experiments. Images were acquired at 60s intervals. Backgrounds were subtracted from fluorescence images. All data were analyzed by Image J software to calculate the emission intensity ratios CFP/YFPSE. For each petri dish, 2–5 cells were observed and data were collected from at least 15 cells for each treatment.

2.7. Statistical analyses

Polarized homo-FRET and cAMP data were expressed as mean ± SEM. Statistical evaluation of mean differences un-treatment and treatments groups was analyzed by one-way ANOVA followed by the Tukey multiple comparison test and Student's *t*-test to compare between two groups using R version 3.3.1. P values $< .05$ were considered statistically significant.

2.8. Ambient temperature EPR measurements

Electron paramagnetic resonance (EPR) was used to record characterize the vanadium complexes formed in DMEM media and aqueous solution. Spectra were recorded at ambient temperature in aqueous solution using a Bruker ESR-300 spectrometer and previously described methods [52]. The solutions were made at 1 mM concentrations and were recorded in 1-mm glass capillary tubes which were placed in 2-mm quartz tubes. A powder sample of 2,2-diphenyl-1-picrylhydrazyl (DDPH, g = 2.0037) was used as an external standard. The spectra were recorded at 9.84 GHz frequency and 20.00 mW microwave power with modulation frequency 100.00 kHz, modulation amplitude 10.00 G, time constant 5.12 ms, sweep width 1000.00 G, sweep time 5.24 s, resolution 1048 points and ten scans with a central field 3511.20 G.

2.9. Speciation calculations

Solution speciation was measured using potentiometry and spectroscopic methods resulting in quantification of species which would be modeled to a defined stoichiometry using formation constants, β [60–70]. Details in the speciation of BMOV have been reported previously [65,70]. In brief, the complexes are defined by the notation (p, q, r). Eq. (4) shows H^+, a metal ion (M^{2+}), and a ligand (L^-) forming a complex with the stoichiometry defined by p, q, and r in an equilibrium reaction, respectively [63,65]. The resulting formation constant β (p, q, r) is shown in Eq. (5), where the concentrations of H^+, M^{2+}, and L^- (which together form the BMOV complex described here) are multiplied with each other and divided by the concentration of the BMOV complex originally added to the solution.

$$pH^+ + qM^{2+} + rL^- \rightarrow (H^+)_p(M^{2+})_q(L^-)_r \quad (4)$$

$$\beta(p,q,r) = \frac{[(H^+)_p(M^{2+})_q(L^-_r)]}{[H^+]^p[M^{2+}]^q[L^-]^r} \quad (5)$$

Because the biological assay was carried out at an ionic strength of 0.17 the parameters used for the calculations where chosen similar to the ionic strength used in the biological assay [69]. The intact coordination complex, BMOV, can described by a series of equations and the associated formation constants that represent the entire system [65–68,70]. Using the reported constants as shown in Table S1, we can describe the species distribution under conditions similar to those of the media.

3. Results

3.1. Studies of fluorescence anisotropy

Prior to initiating homo-FRET studies, growth inhibition viability assays were performed using a resazurin-based bioreductive fluorometric assay to determine the concentrations used in the following studies. The concentrations studied were 100, 50, 10, 5,1 μM. Results are shown in Fig. S1 in Supplemental information. The IC_{50} values for BMOV, BEOV and $VOSO_4$ measured were 34, 34 and 65 μM, respectively (Supplemental information). These data show that BMOV and BEOV are 2-fold more toxic to the cells than $VOSO_4$, a result that indicates that BMOV and BEOV remain at least partially intact under these experimental conditions. Speciation studies discussed below verify this expectation. Because homo-FRET studies on cells are of most interest at non-toxic concentrations, we chose to use 10 μM for the rest of the studies presented in this work.

The effects of BMOV, BEOV and $VOSO_4$ on the initial anisotropy were measured using homo-transfer FRET methods. Two strategies were used. The first series of experiments assessed the initial anisotropy for BMOV-, BEOV- and $VOSO_4$-treated cell lines expressing < 9 k, 10–30 k, 35–80 k or > 85 k LHR per cell (Fig. 3). The second strategy was to examine the relationship between initial anisotropy and fluorescence intensity on a per cell basis (Fig. 4). Anisotropy values were obtained at each time point for a total of 30 measurements from time 0–15 min after initiating photobleaching for each cell examined. As eYFP on each cell is photobleached, there is a decrease in fluorescence intensity and an increase in measured anisotropy. Hypothetically, after photobleaching eYFP until there is one remaining eYFP per cell, the fluorescence intensity has decreased to a value near zero and, because there are no eYFP molecules available for polarized homo-FRET, the anisotropy has increased to its maximum value of 0.38.

Values for initial fluorescence anisotropy are shown in Fig. 3 for cell lines expressing < 9 k, 10-30 k, 35-80 k or > 85 k LHR-eYFP per cell. Untreated cells had initial anisotropy values of 0.20 ± 0.01, 0.13 ± 0.01, 0.09 ± 0.01, and 0.06 ± 0.01, respectively. For cells expressing < 9 k, 10–30 k, or 35–80 k LHR, treatment of cells with either 100 nM hCG for 1 h or 10 μM BMOV, BEOV and $VOSO_4$ for 12 h reduced the initial anisotropy values significantly. The greatest reductions, to approximately half the initial anisotropy seen for untreated cells, occurred when cells expressed < 9 K LHR receptors per cell and suggested that there was significant clustering of LHR per cell in response to 100 nM hCG, 10 μM BMOV, 10 μM BEOV or 10 μM $VOSO_4$. Reductions in initial anisotropy were less pronounced for cells with 10-

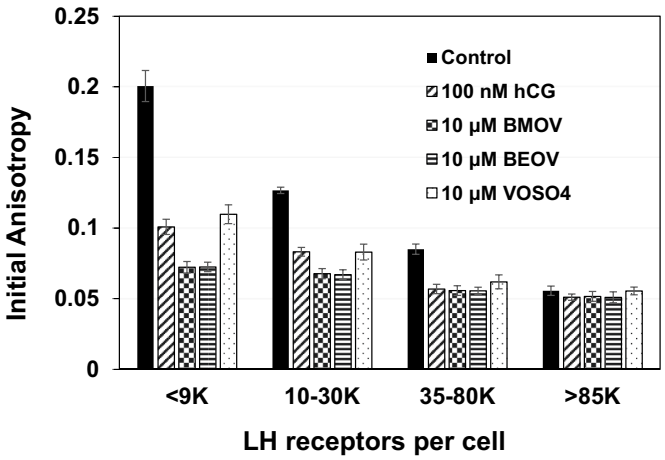

Fig. 3. The effects of LHR numbers per cell on the initial anisotropy values for LHR-eYFP in the absence (control) or presence of hCG or on cells treated with vanadium compounds. Data shown are the mean and S.E. of 25–43 individual measurements depending on the particular treatment.

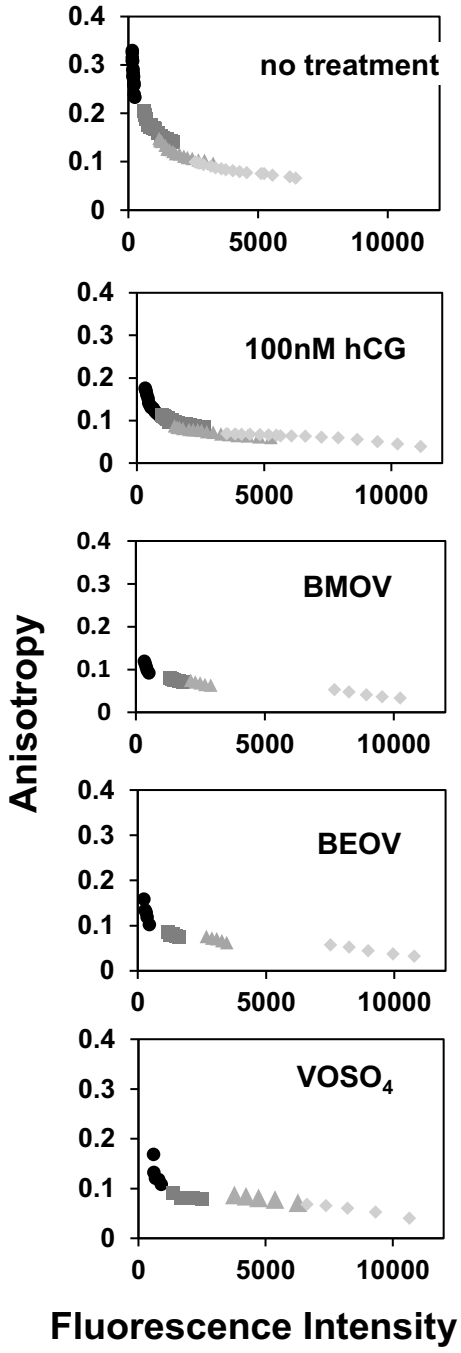

Fig. 4. Anisotropy versus fluorescence intensity of untreated cells and for cells treated with 100 nM hCG, BMOV, BEOV or $VOSO_4$. As discussed in Materials and Methods, LHR-eYFP on individual cells was photobleached for 15 min cells. Anisotropy and the fluorescence signal were measured at 1 min intervals. Each anisotropy value was plotted versus measured fluorescence intensity. Measurements were obtained from cells expressing < 9 k, 10–30 k, 35–80 k and > 85 k LHR per cell. Data shown were obtained from 8–15 measurements on individual cells.

30 k or 35–80 k LHR per cell but were statistically significant. As is the case for cells lines expressing < 9 k LHR, these receptors on these cell lines also underwent some degree of clustering with exposure to hCG, BMOV, BEOV or $VOSO_4$. Interestingly, the cell line with > 85 k LHR per cell, exhibited no change in anisotropy with hCG, BMOV, BEOV or $VOSO_4$ treatment. The initial anisotropy of untreated cells in this cell line was already low, 0.06 ± 0.01, and not affected by hormone or vanadium compound exposure. These results suggest that these LHR are already present in comparatively large clusters and do not cluster further with hormone or vanadium compound exposure.

Fig. 4 shows the relationship between measured levels of fluorescence and anisotropy for individual cells. Untreated cells with low levels of fluorescence, exhibit values for anisotropy that approach the theoretical maximum value of 0.38. These values are likely to represent receptor monomers or dimers on the cell membrane. As values for fluorescence intensity per cell increase, the values for anisotropy decrease. Cells with more eYFP contributing to increased values for fluorescence intensity, have lower values for anisotropy which represent receptors clustered in larger structures. For cells treated with 100 nM hCG, 10 μM BMOV, 10 μM BEOV or 10 μM $VOSO_4$, low values for fluorescence intensity are accompanied by low values for anisotropy suggesting that there are larger cluster sizes resulting from exposure to hormone or vanadium compounds on these cells.

3.2. Studies of intracellular cAMP levels

There is a comparatively simple relationship between anisotropy values discussed above and intracellular levels of cAMP. Receptors that are extensively clustered, either from binding of hCG or exposure of cells to vanadium compounds, are also actively signaling. If we consider cells expressing < 9 k LHR per cell, this relationship is apparent. Untreated receptors exhibit high values for initial anisotropy (Fig. 3) and have low basal levels of intracellular cAMP as indicated by a ratio of CFP/YFPSE which is low (Fig. 5). Treating cells with either 100 nM hCG or 10 μM BMOV, BEOV and $VOSO_4$ for 15 min increases intracellular cAMP. Under these conditions (Fig. 3), anisotropy values decrease, indicating receptor aggregation. Basal levels of intracellular cAMP in untreated cells increase with increasing numbers of LHR per cell. These increased levels of cAMP per cell are associated with decreasing initial anisotropies. When cells overexpress LHR, as for example, when cells express > 85 k receptors per cell, the addition of 100 nM hCG or 10 μM BMOV, BEOV and $VOSO_4$ has no effect on intracellular cAMP levels which are already high. These receptors are preclustered and, as a result, constitutively active.

It is possible to verify that over-expressed LHR are constitutively active as shown in Fig. 6. Forskolin activates adenylate cyclase [71] and is used to demonstrate the maximum level of cAMP production possible

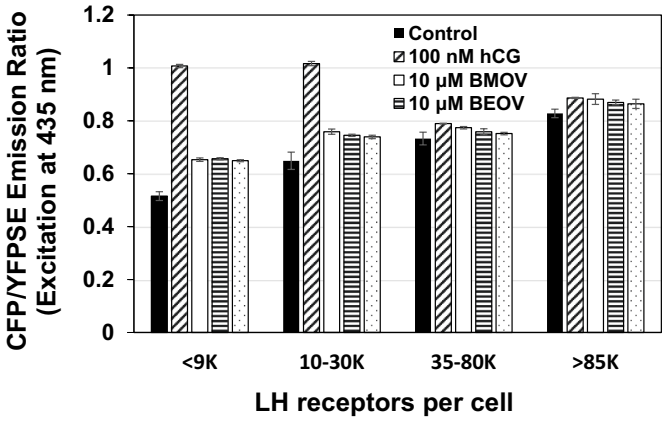

Fig. 5. The effects of LHR numbers per cell on intracellular cAMP levels in the absence (control) or presence of 100 nM hCG or on cells treated with various vanadium compounds. ICUE3 was used as a cAMP reporter molecule. When there is an increase in intracellular cAMP, cAMP binds to ICUE3 and reduces energy transfer between CFP and YFP (YFPSE) upon exposure of ICUE3 to 435 nM light. This increases the CFP/YFPSE ratio as shown in this figure. In the absence of cAMP, there is increased energy transfer from CPF to YFP and thus an increase in sensitized emission by YFP which reduces the CFP/YFPSE ratio. Data shown are the mean and S.E. of 25–43 individual measurements depending on the particular treatment.

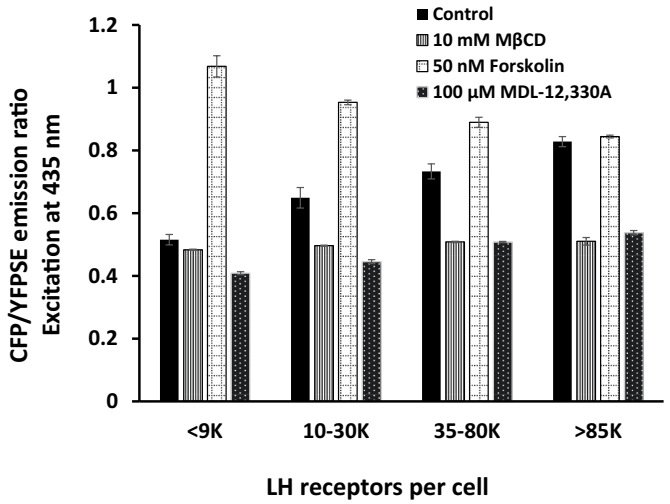

Fig. 6. cAMP levels were measured in cells treated with MβCD, a compound that extracts cholesterol from plasma membrane rafts and disrupts their structure. Also shown are effects of forskolin, which maximally activates adenylate cyclase in cells, and MDL-12,330A, an adenylated cyclase inhibitor. Forskolin treatment of cells expressing > 85 k LHR per cell demonstrates that receptors are constitutively active and that forskolin is unable to further activated adenylate cyclase in these cells. Nevertheless, adenylate cyclase activity can be inhibited by MDL-12,330A to levels which are comparable to basal levels of cAMP observed in cells with < 9 k LHR per cell where LHR is not constitutively active. Data shown are the mean and S.E. of 13–40 individual measurements depending on the particular treatment.

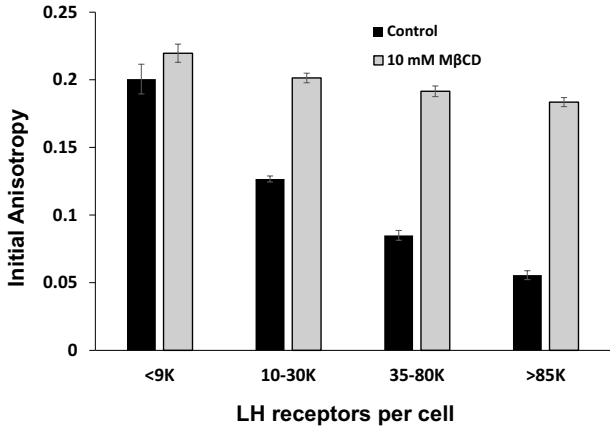

Fig. 7. LHR receptors are localized in plasma membrane rafts when receptor numbers per cell are high. As shown for cells expressing > 85 k LHR per cell, disruption of rafts results in an increase in initial anisotropy and suggests that the raft localized receptors were extensively clustered in rafts and disperse upon disruption of raft microdomains. For cells expressing < 9 k LHR per cell, disruption of raft structures has no effect on initial anisotropy suggesting that these receptors are present in the bulk membrane and are not extensively aggregated. Data shown are the mean and S.E. of 25–42 individual measurements depending on the particular treatment.

in a cell. As shown in Fig. 6, < 9 k, 10–30 k, 35–80 k or > 85 k LHR per cell have increasing levels of intracellular cAMP per cell. Forskolin treatment of these cells (50 nM) causes an increase in cAMP levels per cell in cells expressing < 9 k, 10–30 k or 35–80 k LHR per cell. For cells expressing > 85 k LHR per cell, adenylate cyclase is maximally functional and there is no further effect of forskolin on cAMP levels. It is also possible to inhibit adenylate cyclase activity using 100 μM MDL-12,330A. When cells express < 9 K LHR per cell, there is little effect of MDL-12,330A on the basal level of cAMP which is already low. When cells express > 85 k LHR per cell, the basal level of cAMP is high due to constitutive activation of LHR by extensively clustered LHR and not affected by adding forskolin. MDL-12,330A treatment reduces the level of cAMP in these cells from 0.82 ± 0.16 to 0 0.538 ± 0.007, which is comparable to the cAMP level in cells expressing < 9 k LHR/cells.

3.3. Effects of disrupting raft microdomains on receptor anisotropy and intracellular cAMP

The final question addressed in these studies is the location of LHR in specialized membrane microdomains such as rafts. Fig. 7 shows the effect of raft disruption using methyl-β-cyclodextrin (MβCD), a chemical agent that, at these concentrations, extracts cholesterol from the cell membrane and disrupts rafts [72]. As shown in Fig. 6, pre-treatment of cells with 10 nM MβCD, reduces intracellular cAMP in cells expressing < 9 k, 10–30 k, 35–80 k or > 85 k LHR to low basal levels characteristic of cells expressing < 9 k LHR. Anisotropy values in these cells lines suggest that LHR, with increasing numbers of LHR, become localized in membrane rafts (Fig. 7). In addition to reducing intracellular cAMP levels, MβCD treatment of cells appears to disrupt those raft structures where receptors are concentrated and disperses receptors into smaller clusters. This is most apparent when cells over-express LHR.

3.4. EPR spectroscopy and speciation

BMOV and BEOV are coordination complexes and, as a result, will undergo hydrolytic reactions in aqueous media [60–62,65,70,73]. We therefore examined the speciation of the system [65–68,70] and specifically the vanadium species forming under experimental conditions during the 15 min incubation of these experiments. The assay treatment does not significantly oxidize or hydrolyze the BMOV or BEOV during the assay and incubation; however, during the 12–24 h treatment some oxidation and hydrolysis will have taken place since the half-life for this compound has been reported to be about 24 h. Indeed, the blue color for $VOSO_4$ diminished upon reduction and can be observed in aqueous solutions. In media the red phenol solution overpowered the color of the aqueous vanadium(IV) solution. Therefore, we monitored the speciation of BMOV and BEOV in the cell culture media using EPR spectroscopy. Our results were found to compare to the stability data reported previously [65,70,73]. As shown in Fig. 8, the spectra for BMOV and BEOV are very similar at pH 7.4 but differ from spectra for the reference $VOSO_4$ sample at pH 4. The chemistry of VO^{2+} in aqueous solution is such that dimers and polymers form at neutral pH, significantly reducing the signal for VO^{2+} as shown in Fig. 8 [6,18,20,65,67,68]. This was confirmed by recording the EPR spectrum of $VOSO_4$ in medium (Table S1 in Supplemental Information). We conclude that both BMOV and BEOV remain partially intact as the 1:2 complex in media during the treatment of the cells; other species are not observable in the EPR spectrum and thus represent no more than the 10–20% of the species observed at 1 mM (spectra were also recorded at 10 mM and are shown in the Supplemental information).

Once BMOV or BEOV interact with cells, it is more difficult to directly measure their speciation. This is further complicated by the fact that BMOV and BEOV will oxidize in the presence of oxygen. This was confirmed by measuring the EPR spectra of an “aged” solution of BMOV and BEOV in cell culture media. The EPR signal in these “aged” samples decreased as a function of time, a result consistent with literature reports stating that the half-life of these compounds is about 24 h [65,70]. These studies support the expectation that part of the complex remains intact; at a concentration of 1 μM, speciation results in about equal amounts of intact and hydrolyzed complex during the initial part of the 12–24 h experiment.

Although we demonstrated that 1.0 mM BMOV and BEOV remain intact in cell culture media, 10 μM BMOV or BEOV was used in the cellular studies. To investigate the speciation expected at 100-fold lower concentrations, we calculated the speciation of BMOV anticipated at 10 μM concentration. The formation constants for BMOV was reported

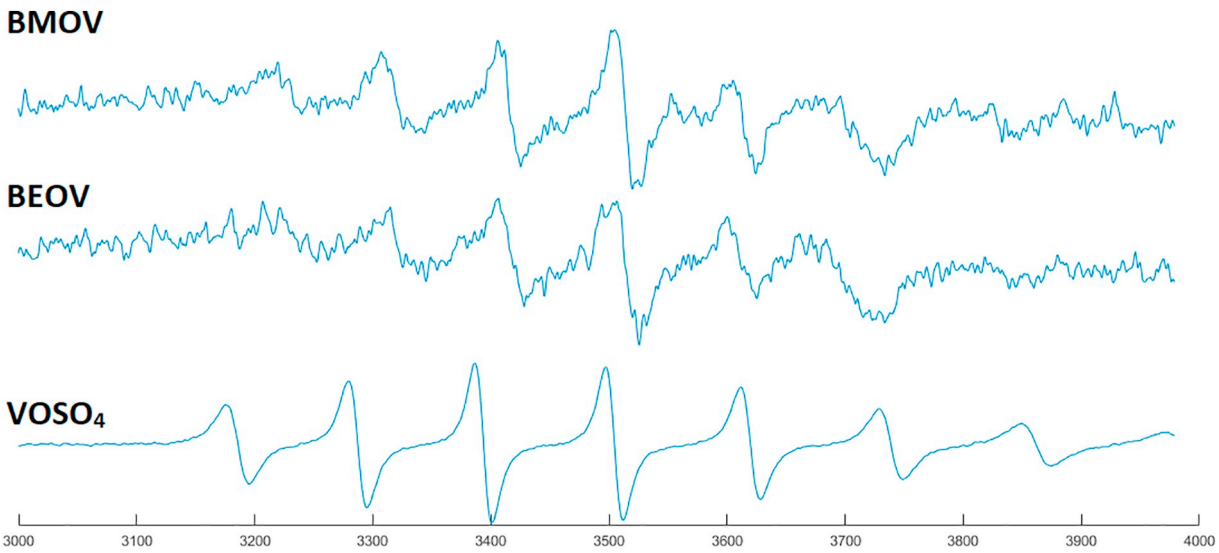

Fig. 8. EPR spectra of 1 mM BMOV and BEOV, respectively in DMEM used for the studies with the LHR (pH 7.4) compared to the reference $VOSO_4$ at pH 4. The spectra are recorded so that they show relative concentration of vanadium(IV) in solution which is less at pH 7.4 than at pH 4 because vanadium(IV) dimerize and oxidize at pH 7.4.

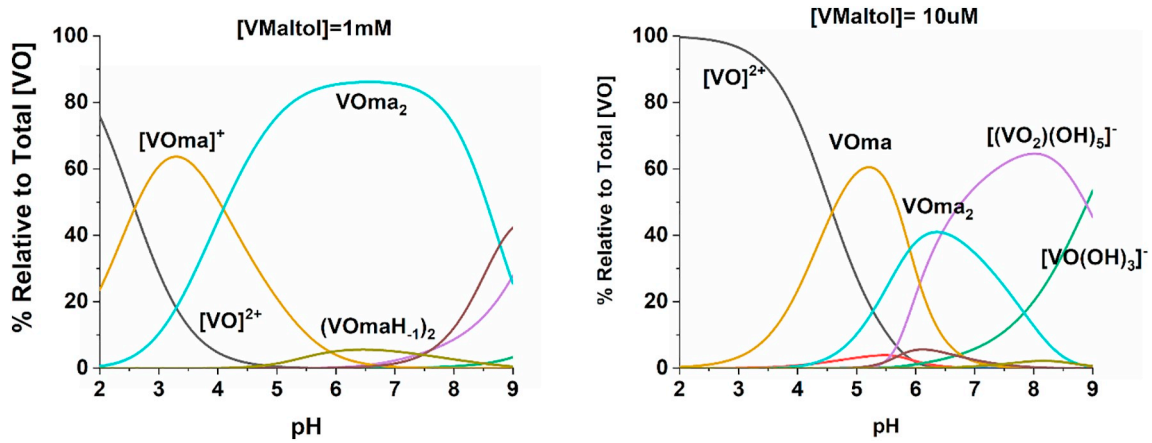

Fig. 9. Distribution diagram of hydrolysis and complexes formed in the VO(IV)-maltol system A (C_{vo} = 1 mM, C_{ma} = 2 mM), B (C_{vo} = 10 uM, C_{ma} = 20 uM).

previously and so was the hydrolysis constants for aqueous V(IV). The speciation curves are shown for 1.0 mM and for 10 μM in Fig. 9. These figures show that at 1.0 mM the major species is indeed the 1:2 species and that both the 1:1 and the VO^{2+} are minor species. These modeled results are consistent with the EPR spectrum presented in Fig. 8. Because the experimental concentration was lower than that used in EPR studies, the contribution of the 1:1 and VO^{2+} species was estimated for a 10 μM concentration using speciation calculations. Indeed, the fraction of the 1:2 BMOV species decreased and the contributions of the other two species increased. In fact, at 10 μM the concentration of the VO^{2+} species increased to a level that is likely to be about 60–65% of the experimental solution and is thus the major species present. The sum of the 1:1 species and BMOV is estimated to be about 35–40% of the solution. However, we found that the observed effects by BMOV and BEOV are 2-fold greater than those of VO^{2+} and thus, because speciation studies confirm that some BMOV remains intact we can attribute the observed effects to BMOV or BEOV. Indeed, these result show that BMOV and accordingly BEOV are more potent than VO^{2+}.

4. Discussion

The work presented suggest that BMOV, BEOV and $VOSO_4$ induce LHRs to form receptor clusters in plasma membrane rafts. The formation of LHR clusters, indicated by a decrease in the initial anisotropies measured in homo-transfer FRET studies, and an increase in intracellular cAMP levels associated with receptor clustering, suggest that these vanadium compounds are involved in cell signaling. As with our previous studies of IR in rat basophilic leukemia cells (RBL-2H3 cells) [31], our data support the hypothesis that vanadium compounds are driving activation of LHR in lipid rafts leading to signal transduction. In studies of IR, both BMOV and insulin showed similar effects on IR lateral diffusion on the cell-surface but, while BMOV induced a marked reduction of cell-surface lipid order, binding of insulin to IR did not have any effect on membrane lipid packing.

Changes in lipid packing in the presence of BMOV, BEOV or $VOSO_4$ are consistent with the idea that cell-surface membrane fluidity is influenced by these compounds. Lipid disorder in CHO cells is increased following treatment with 10 μM BMOV, BEOV or $VOSO_4$ and disrupting the integrity of lipid rafts by extracting cholesterol from membranes using MβCD causes an even greater increase in lipid disorder, a result similar to that reported by Winter et al. [31] in RBL-2H3 cells. The use of Di-4-ANEPPDHQ for both the measurement of membrane fluidity and the identification of cholesterol enriched domains has been established [74,75] and has been shown to be a powerful tool for probing membrane fluidity in live cells specifically when compared to existing probes [76]. It should be noted our results on the effects of BMOV on

membrane lipid packing, i.e., fluidity, differ from those of Yang et al. [77] who evaluated lipid fluidity in red blood cell membranes treated with various vanadium-containing compounds. They demonstrated that, to varying degrees, several compounds including $NaVO_3$, VO $(acac)_2$, BMOV, and $[VO_2dipic]^-$, decreased membrane fluidity and increase lipid order.

As with studies of insulin effects on cells treated with BMOV, we cannot rule out secondary effects of vanadium compounds on protein phosphatases that lead to, or support, LHR-mediated signaling in response to BMOV, BEOV or $VOSO_4$. However, if BMOV, BEOV or $VOSO_4$ effects on phosphatases are involved in activation of LHR, a G-protein coupled receptor, the phosphatases involved are likely to be different from those involved in activation IR, a tyrosine kinase receptor. Nonetheless, it is clear that vanadium compounds can affect expression of genes for enzyme in cells. Studies using VO-dipic-Cl showed lipid abnormalities in streptozotocin (STZ)-induced diabetic rats were alleviated [78]. Specifically, the down regulation of a number of proteins (the peroxisome proliferator-activator receptor, the CCAAT element binding protein, the sterol regulatory element binding protein, fatty acid synthases (FAS) and fatty acid-binding protein 4 (FABP4) [79]. In addition, up-regulation of acetyl coenzyme A carboxylase, adenosine monophosphate-activated protein kinase (AMPK) and liver kinase B1 (LKB1) was observed in a dose-dependent manner. Furthermore, VOdipic-Cl was able to induce AMPK small interfering RNA to markedly up-regulate C/EBP alpha, PPAR gamma, FAS and FABP4 expression. Together these studies showed that VOdipic-Cl can inhibit 313-L1 preadipocyte differentiation and adipogenesis through activating the LKB1/AMPK-dependent signaling pathway [79]. Although any or all of these pathways may be involved in BMOV, BEOV or $VOSO_4$ effects on CHO cell membranes and LHR signaling, it appears that alterations in the lipid bilayer contribute most directly to the concentration of IR or LHR in lipid rafts where they initiate signaling via their respective signal transduction pathways.

Together these results indicate that a new and novel method for activation of membrane proteins may involve indirect effects on the protein lipid environment resulting from direct effects of vanadium compounds on membrane lipid packing. It remains to be determined whether this is a general mechanism for plasma membrane proteins that use raft domains for cell signaling [80]. Nevertheless, such a mechanism may have important pharmacological implications for G protein-coupled receptors such as the β-adrenergic receptor or the μ-opioid receptor which, like LHR, undergo extensive clustering upon binding ligand and signal in raft domains (reviewed in [80]). Vanadium compounds are, at a minimum, useful tools in the study of the spatio-temporal relationship involved in signal transduction, a relationship that by necessity involves the membrane lipid bilayer and offers an additional layer of complexity to signal transduction mechanism used by plasma membrane receptors.

5. Conclusions

When cells expressed < 9 k LHRs per cell, receptors, prior to hormone treatment or exposure to vanadium compounds were present in small clusters, perhaps as dimers or trimers. Binding of hCG to its receptor increased the size of LHR clusters as indicated by a decrease in the initial anisotropy measured in homo-transfer FRET measurements and receptors began to signal productively as indicated by an increase in intracellular cAMP. Similarly, BMOV, BEOV and $VOSO_4$ treatments decreased values for initial anisotropy and cAMP signal was initiated without addition of hormone. When cells express > 85 k LHRs per cell, LHRs are in large clusters in the absence of hCG and, because these receptors are constitutively active, intracellular cAMP levels are high. Treating cells with hCG or the various vanadium compounds does not affect either the aggregation state of LHRs or further elevate intracellular cAMP. BMOV, BEOV and $VOSO_4$ have effects similar to those of hCG on LHR signal transduction at low receptor concentration on the membrane.

The effects of BMOV, BEOV and $VOSO_4$ on LHR signal transduction do not affect the function of adenylate cyclase, the enzyme that catalyzes cAMP synthesis. Furthermore, forskolin treatment at a concentration sufficient to maximally activate adenylate cyclase [71], does not further elevate levels of intracellular cAMP in cells treated with hCG or BMOV, BEOV and $VOSO_4$. The cAMP producing enzyme can however be inhibited with MDL-12,330a hydrochloride, an adenylate cyclase inhibitor [81]. Vanadium compounds, unlike hCG, have been shown to interact with lipid monolayers (see Fig. 2). Although some vanadium compounds such as BMOV do not fully insert in the lipid monolayer [48], their interactions with the monolayer are sufficient to decrease lipid order in CHO cell membranes (see Fig. S2 in Supplemental information). Furthermore, BMOV perturbs the distribution of membrane proteins such as the insulin receptor [82] between the bulk membrane and plasma membrane rafts. Receptors move into the raft domains and initiate signal transduction. The action of vanadium compounds is likely to occur through its effects on lipid order.

LHRs, like insulin receptors, use raft domains as signaling platforms [35]. These studies indicate that the initial organization of receptors in the membrane prior to binding of ligand or exposure to BMOV/BEOV or $VOSO_4$ involves raft domains when receptors are overexpressed and are constitutively active. Thus, when receptor numbers are low, < 9 k LHR per cell, neither receptor cluster size nor intracellular cAMP levels, are affected by disruption of rafts. When the number of LHRs per cell increases to 10–30 k LHR per cell, disruption of raft domains by MβCD causes both an increase in LHR initial anisotropy and a decrease in intracellular cAMP levels. In summary, accumulation of LHR in raft domains results from treating CHO cells with vanadium compounds.

Speciation calculations were done to estimate the concentration of the intact BMOV and BEOV complexes during the experiments where much lower concentrations were used. Because BEOV has similar properties to BMOV, we used it to estimate speciation in similar studies. This is consistent with the fact that we found that the complexed vanadium in the form of either BMOV or BEOV are more effective in inducing the observed response. It follows that greater observed effects are induced by solutions containing vanadium at least partially in the form of BMOV and BEOV. This is because the complexed molecules are more potent than simple vanadyl sulfate. BMOV and BEOV remain at least partially intact over the time course of experiments using CHO cells and are more effective than $VOSO_4$.

Abbreviations

BMOV	bis(maltolato)oxovanadium(IV)
BEOV	bis(ethylmaltolato)oxovanadium(IV)
cAMP	cyclic adenosine monophosphate
CFP	cyan fluorescent protein
DMEM	Dulbecco's modified Eagle medium
EPR	electron paramagnetic resonance
eYFP	enhanced yellow fluorescent protein
FRET	fluorescence resonance energy transfer
Homo-FRET	polarized homo-transfer fluorescence resonance energy transfer
hCG	human chorionic gonadotropin
IR	insulin receptor
LHR	luteinizing hormone receptor
MβCD	methyl beta cyclodextrin
$VOSO_4$	vanadyl sulfate
YFPSE	yellow fluorescent protein sensitized emission

Acknowledgements

D.A. would like to thank King Faisal University and the Saudi Arabian Cultural Mission for her fellowship to study at Colorado State University. D.C.C. would like to thank the Arthur P. Cope Scholar fund administered by the American Chemical Society, USA and the National Science Foundation, USA (CHE-1709564) for partial funding supporting this project.

Declaration of competing interest

The authors have no conflict of interests with regard to this work.

Appendix A. Supplementary data

Supplementary data to this article can be found online at https://doi.org/10.1016/j.jinorgbio.2019.110873.

References

[1] J.C. Pessoa, S. Etcheverry, D. Gambino, Coord. Chem. Rev. 301 (2015) 24–48.
[2] D.C. Crans, J. Org. Chem. 80 (2015) 11899–11915.
[3] G.R. Willsky, L.-H. Chi, M. Godzala, P.J. Kostyniak, J.J. Smee, A.M. Trujillo, J.A. Alfano, W. Ding, Z. Hu, D.C. Crans, Coord. Chem. Rev. 255 (2011) 2258–2269.
[4] M.M. Harding, G. Mokdsi, Curr. Med. Chem. 7 (2000) 1289–1303.
[5] D.C. Crans, L. Henry, G. Cardiff, B.I. Posner, Met. Ions Life Sci. 19 (2019) 203–230.
[6] T. Jakusch, T. Kiss, Coord. Chem. Rev. 351 (2017) 118–126.
[7] T. Scior, J. Antonio Guevara-Garcia, Q.-T. Do, P. Bernard, S. Laufer, Curr. Med. Chem., 23, 2016, 2874–2891.
[8] K.H. Thompson, C. Orvig, J. Inorg. Biochem. 100 (2006) 1925–1935.
[9] H. Sakurai, Y. Kojima, Y. Yoshikawa, K. Kawabe, H. Yasui, Coord. Chem. Rev. 226 (2002) 187–198.
[10] D.C. Crans, L. Yang, A. Haase, X. Yang, Met. Ions Life Sci 18 (2018) 251–279.
[11] I. Esteban Leon, J. Fernando Cadavid-Vargas, A. Laura Di Virgilio, S. Beatriz Etcheverry, Curr. Med. Chem. 24 (2017) 112–148.
[12] E. Kioseoglou, S. Petanidis, C. Gabriel, A. Salifoglou, Coord. Chem. Rev. 301 (2015) 87–105.
[13] A. Bishayee, A. Waghray, M.A. Patel, M. Chatterjee, Cancer Lett. 294 (2010) 1–12.
[14] D. Gambino, Coord. Chem. Rev. 255 (2011) 2193–2203.
[15] D.A. Barrio, S.B. Etcheverry, Curr. Med. Chem. 17 (2010) 3632–3642.
[16] S.L. Calixto, N. Glanzmann, M.M.X. Silveira, J. da Trindade Granato, K.K.G. Scopel, T.T. de Aguiar, R.A. DaMatta, G.C. Macedo, A.D. da Silva, E.S. Coimbra, Chem. Biol. Interact. 293 (2018) 141–151.
[17] M. Aureliano, C.A. Ohlin, J. Inorg. Biochem. 137 (2014) 123–130.
[18] D.C. Crans, J.J. Smee, E. Gaidamauskas, L. Yang, Chem. Rev. 104 (2004) 849–902.
[19] T. Kiss, É.A. Enyedy, T. Jakusch, O. Dömötör, Curr. Med. Chem. 26 (2019) 580–606.
[20] T. Jakusch, J.C. Pessoa, T. Kiss, Coord. Chem. Rev. 255 (2011) 2218–2226.
[21] J.L. Domingo, M. Gómez, Food Chem. Tox. 95 (2016) 137–141.
[22] G.R. Willsky, K. Halvorson, M.E. Godzala III, L.-H. Chi, M. Most, P. Kaszynski, C.C. Dl, A.B. Goldfine, P.J. Kostnyniak, Metallomics 5 (2013) 1491–1502.
[23] K.H. Thompson, C. Orvig, J. Inorg. Biochem. 100 (2006) 1925–1935.
[24] K.H. Thompson, J. Lichter, C. LeBel, M.C. Scaife, J.H. McNeill, C. Orvig, J. Inorg. Biochem. 103 (2009) 554–558.
[25] S. Treviño, A. Díaz, E. Sánchez-Lara, B.L. Sanchez-Gaytan, J.M. Perez-Aguilar, E. González-Vergara, Biol. Trace Elem. Res. 188 (2019) 68–98.
[26] E. Bellomo, K.B. Singh, A. Massarotti, C. Hogstrand, W. Maret, Coord. Chem. Rev. 327 (2016) 70–83.
[27] L. Lu, M. Zhu, Antioxid. Red. Signal. 20 (2014) 2210–2224.
[28] C.G. Azevedo, I. Correia, M.M. dos Santos, M.F. Santos, T. Santos-Silva, J. Doutch, L. Fernandes, H.M. Santos, J.L. Capelo, J.C. Pessoa, J. Inorg. Biochem. 180 (2018) 211–221.
[29] I.E. Leon, A.L. Di Virgilio, V. Porro, C.I. Muglia, L.G. Naso, P.A.M. Williams, M. Bollati-Fogolin, S.B. Etcheverry, Dalton Trans. 42 (2013) 11868–11880.
[30] U. Jungwirth, C.R. Kowol, B.K. Keppler, C.G. Hartinger, W. Berger, P. Heffeter, Antioxid. Red. Signal. 15 (2011) 1085–1127.
[31] P.W. Winter, A. Al-Qatati, A.L. Wolf-Ringwall, S. Schoeberl, P.B. Chatterjee, B.G. Barisas, D.A. Roess, D.C. Crans, Dalton Trans. 41 (2012) 6419–6430.
[32] Z. Salamon, G. Tollin, I. Alves, V. Hruby, Method. Enzymol. 461 (2009) 123–146.
[33] I.D. Alves, S. Lecomte, Acc. Chem. Res. 52 (2019) 1059–1067.
[34] K. Simons, E. Ikonen, Nature 387 (1997) 569–572.
[35] A.L. Wolf-Ringwall, P.W. Winter, J. Liu, A.K. Van Orden, D.A. Roess, B.G. Barisas, J. Biol. Chem. 286 (2011) 29818–29827.
[36] C.J. Philpott, N.A. Rahman, T.R. Londo, D.A. Roess, Biol. Reprod. 46 (Supplement 1) (1992) 63.
[37] M. Hunzicker-Dunn, G. Barisas, J. Song, D.A. Roess, J. Biol. Chem. 278 (2003) 42744–42749.
[38] D. Holowka, E.D. Sheets, B. Baird, J. Cell Sci. 113 (2000) 1009–1019.
[39] M.P. Czech, Nature 407 (2000) 147.
[40] M. Kanzaki, J.E. Pessin, Curr. Biol. 13 (2003) R574–R576.
[41] S.J. Singer, G.L. Nicolson, Science 175 (1972) 720–731.
[42] G.D. Niswender, D.A. Roess, H.R. Sawyer, W.J. Silvia, B.G. Barisas, Endocrinology 116 (1985) 164–169.
[43] R.D. Horvat, S. Nelson, C.M. Clay, B.G. Barisas, D.A. Roess, Biochem. Biophys. Res. Comm. 255 (1999) 382–385.
[44] J. Stover, C.D. Rithner, R.A. Inafuku, D.C. Crans, N.E. Levinger, Langmuir 21 (2005) 6250–6258.
[45] D.C. Crans, C.D. Rithner, B. Baruah, B.L. Gourley, N.E. Levinger, J. Amer. Chem. Soc. 128 (2006) 4437–4445.
[46] D. Roess, S.L. Smith, A.A. Holder, B. Baruah, A.M. Trujillo, D. Gilsdorf, M.L. Stahla, D.C. Crans, Vanadium: the versatile metal, ACS Symp. Ser. 711 (2007) 121–134.
[47] D.A. Roess, S.M.L. Smith, P. Winter, J. Zhou, P. Dou, B. Baruah, A.M. Trujillo, N.E. Levinger, X. Yang, B.G. Barisas, D.C. Crans, Chem. Biodivers. 5 (2008) 1558–1570.
[48] D.C. Crans, S. Schoeberl, E. Gaidamauskas, B. Baruah, D.A. Roess, J. Biol. Inorg. Chem. 16 (2011) 961–972.
[49] A. Al-Qatati, P. Winter, A. Wolf-Ringwall, P. Chatterjee, A. Van Orden, D. Crans, D. Roess, B. Barisas, Cell Biochem. Biophys. (2012) 1–10 Humana Press Inc..
[50] A. Al-Qatati, F.L. Fontes, B.G. Barisas, D. Zhang, D.A. Roess, D.C. Crans, Dalton Trans. 42 (2013) 11912–11920.
[51] A.G. Sostarecz, E. Gaidamauskas, S. Distin, S.J. Bonetti, N.E. Levinger, D.C. Crans, Chem. Eur. J. 20 (2014) 5149–5159.
[52] S.S. Amin, K. Cryer, B. Zhang, S.K. Dutta, S.S. Eaton, O.P. Anderson, S.M. Miller, B.A. Reul, S.M. Brichard, D.C. Crans, Inorg. Chem. 39 (2000) 406–416.
[53] A. Levina, D.C. Crans, P.A. Lay, Coord. Chem. Rev. 352 (2017) 473–498.
[54] Y. Lei, G. Hagen, S. Smith, J. Liu, B.G. Barisas, D. Roess, Mol. Cell. Endocrinol. 260–262 (2007) 65–72.
[55] D.W. Piston, G.-J. Kremers, Trends Biochem. Sci. 32 (2007) 407–414.
[56] J.A. Dix, A. Verkman, Biophys. J. 57 (1990) 231–240.
[57] A.H. Clayton, Q.S. Hanley, D.J. Arndt-Jovin, V. Subramaniam, T.M. Jovin, Biophys. J. 83 (2002) 1631–1649.
[58] S. Ganguly, A.H.A. Clayton, A. Chattopadhyay, Biophys. J. 100 (2011) 361–368.
[59] D. Zhang, G.E. Hadhoud, K. Helm, D.A. Roess, B.G. Barisas, J. Fluores. 29 (2019) 53–60.
[60] T. Kiss, T. Jakusch, D. Hollender, Á. Dörnyei, É.A. Enyedy, J.C. Pessoa, H. Sakurai, A. Sanz-Medel, Coord. Chem. Rev. 252 (2008) 1153–1162.
[61] T. Jakusch, D. Hollender, É. Enyedy, C.S. González, M. Montes-Bayón, A. Sanz-Medel, J. Costa Pessoa, I. Tomaz, T. Kiss, Dalton Trans. (2009) 2428–2437.
[62] K. Tamás, O. Akira, Bull. Chem. Soc. 80 (2007) 1691–1702.
[63] D.C. Crans, K.A. Woll, K. Prusinskas, M.D. Johnson, E. Norkus, Inorg. Chem. 52 (2013) 12262–12275.
[64] D. Rehder, J. Inorg. Biochem. 147 (2015) 25–31.
[65] A.G. Baró, I. Andersson, L. Pettersson, A. Gorzsás, Dalton Trans. (2008) 1095–1102.
[66] L.V. Boas, Pessoa JC, in: G.W (Ed. (Ed.), Compreh. Coord. Chem., 5, 1987.
[67] J. Pessoa, I. Tomaz, T. Kiss, E. Kiss, P. Buglyó, J. Biol. Inorg. Chem. 7 (2002) 225–240.
[68] J. Costa Pessoa, J. Inorg. Biochem. 147 (2015) 4–24.
[69] A. Bergeron, K. Kostenkova, M. Selman, H.A. Murakami, E. Owens, N. Haribabu, R. Arulanandam, J.-S. Diallo, D.C. Crans, BioMetals (2019) 1–17.
[70] C. Orvig, P. Caravan, L. Gelmini, N. Glover, F.G. Herring, H. Li, J.H. McNeill, S.J. Rettig, I.A. Setyawati, J. Amer. Chem. Soc. 117 (1995) 12759–12770.
[71] K.B. Seamon, W. Padgett, J.W. Daly, Proc. Nat. Acad. Sci. 78 (1981) 3363–3367.
[72] S. Mahammad, I. Parmryd, Biochem. Biophys. Acta - Biomembranes 2008 (1778) 1251–1258.
[73] P. Buglyó, E. Kiss, I. Fábián, T. Kiss, D. Sanna, E. Garribba, G. Micera, Inorg. Chim. Acta 306 (2000) 174–183.
[74] L. Jin, A. Millard, J. Wuskell, H. Clark, K. Loew, Biophys. J. 90 (2005) 2563–2575.
[75] L. Jin, A.C. Millard, J.P. Wuskell, X. Dong, D. Wu, H.A. Clark, L.M. Loew, Biophys. J. 90 (2006) 2563–2575.
[76] Y. Wang, G. Jing, S. Perry, F. Bartoli, S. Tatic-Lucic, Optics Exp 17 (2009) 984–990 OSA.
[77] X. Yang, K. Wang, J. Lu, D.C. Crans, Coord. Chem. Rev. 237 (2003) 103–111.
[78] G.R. Willsky, L.-H. Chi, Y. Liang, D.P. Gaile, Z. Hu, D.C. Crans, Physiol. Genomics 26 (2006) 192–201.
[79] L. Zhang, Y. Huang, F. Liu, F. Zhang, W. Ding, J. Inorg. Biochem. 162 (2016) 1–8.
[80] X. Cheng, J.C. Smith, Chem. Rev. 119 (2019) 5849–5880.
[81] M.G. Palfreyman, M.W. Dudley, H.C. Cheng, A.K. Mir, S. Yamada, W.R. Roeske, T. Obata, H.I. Yamamura, Biochem. Pharmacol. 38 (1989) 2459–2465.
[82] P.W. Winter, A. Al-Qatati, A.L. Wolf-Ringwall, S. Schoeberl, P.B. Chatterjee, B.G. Barisas, D.A. Roess, D.C. Crans, Dalton Trans. 41 (2012) 6419–6430.